Acta Cryst. (1982). B**38**, 1518–1525

Crystals Exhibiting Disorder – The Orthorhombic Polymorph of 9-Bromo-10-methylanthracene

BY T. R. WELBERRY, RAYMOND D. G. JONES AND JOEL EPSTEIN

Research School of Chemistry, Australian National University, Canberra, ACT 2600, Australia

(*Received* 29 *September* 1981; *accepted* 3 *December* 1981)

Abstract

The crystal structure of the orthorhombic polymorph of $C_{15}H_{11}Br$, $M_r = 271{\cdot}16$, has been determined from X-ray (Mo $K\alpha$ radiation) diffraction data. The compound crystallizes in the space group $P2_12_12_1$ with $a = 17{\cdot}439\ (2)$, $b = 16{\cdot}039\ (2)$, $c = 3{\cdot}9590\ (4)$ Å, $U = 1107{\cdot}4$ Å^3, $Z = 4$, $d_c = 1{\cdot}63$ Mg m^{-3}, $F(000) = 544$, λ(Mo $K\alpha$) = 0·71069 Å, μ(Mo $K\alpha$) = 3·894 mm^{-1}. Refinement led to R and wR values of 0·139 and 0·055 for 1651 reflections (0·051 and 0·046 for reflections with $I > 2{\cdot}3\sigma_I$). The 9,10 substituents show disorder of Br and CH_3, the substituent being occupied on average by 0·613 Br and 0·387 C and *vice versa* for the 10 substituent. Additionally, diffuse X-ray scattering has been recorded and interpreted by comparison with optical-analogue models and computed intensities. The results reveal short-range ordering between adjacent molecules when the contact involves a methyl or Br in both molecules. It is shown that two types of contact are involved and for both of these the short-range order reduces the proportion of Br—Br contacts in favour of Br—C contacts, relative to those expected for a random distribution.

Introduction

We have described in an earlier paper (Jones & Welberry, 1980) our interest in binary mixed crystals. In particular, we outlined reasons for the choice of polycyclic aromatic rings and substituent groups. In a subsequent publication (Welberry & Jones, 1980), we showed how optical-diffraction analogues could be used to assist in the interpretation of the diffuse X-ray scattering from such disordered molecular crystals. In these earlier papers our attention was largely focused on the monoclinic or rhomb-shaped polymorph of 9-bromo-10-methylanthracene (BMAR), while in this paper we describe the disordered structure of the orthorhombic or needle-shaped polymorph (BMAN).

A two-dimensional study of BMAN has previously been reported (Prat, 1961) but since it is one of our aims to relate the details of the disorder to intermolecular forces we required more accurate structural parameters including a determination of the occupancy factor for the disordered sites. Hence, in addition to a study of the diffuse X-ray scattering we have undertaken a conventional determination of the 'average' crystal structure using three-dimensional diffractometer data.

Experimental

BMA was prepared by the method of Heller & Schmidt (1971). BMAN crystals of poor quality crystallized from the same concentrated solutions in petroleum ether (b.p. 333–353 K) as the previously reported BMAR crystals. However, crystallization from petroleum ether (b.p. 373–393 K) yielded yellow needle-shaped crystals of BMAN of much better quality with well developed faces {100} and {120}.

Structural-data collection

A crystal 0·22 × 0·26 × 0·34 mm was used to determine the cell dimensions and measure the intensities on a Picker four-circle diffractometer. Cell dimensions were obtained by least squares from the 2θ values of 12 high-angle reflections. Intensities were collected by the θ–2θ continuous-scan method with graphite-monochromated Mo $K\alpha$ radiation. The scan width was 1·8°, extended for the α_1,α_2 splitting, and stationary background counts were taken at the scan limits. Three standard reflections were periodically monitored. The mean deviation of any standard from its mean was 1%. One octant of data was collected to $2\theta = 60°$.

Intensities were corrected for background, absorption and the Lorentz–polarization factor. For each reflection, the variance, σ_I^2, was determined from $\sigma_I^2 = [\sigma_C^2 + \sigma_A^2 + (0{\cdot}01I)^2]$ where σ_C is due to counting statistics, σ_A is due to absorption (Elcombe, Cox, Pryor & Moore, 1971) and I is the net intensity. If $I < 0$, it was set to zero and given zero weight. 1651 unique reflections were measured of which 981 had $I > 2{\cdot}3\sigma_I$.

0567-7408/82/051518-08$01.00

Structure solution and refinement

The coordinates taken from Prat (1961) were taken as a starting point for least-squares refinement using the subset of 981 data. An overall scale factor, atomic coordinates, thermal parameters (isotropic initially for C, Br and ring H atoms, then anisotropic for C and Br), and an occupancy factor for Br in the Br/C(methyl) site were refined to an $R = \sum (|F_o| - k|F_c|)/\sum |F_o|$ of 0·055. Unit weights were used and the function minimized was $\sum w(|F_o| - k|F_c|)^2$. Subsequent refinement was with all data (Moore, 1972) and experimental weights $w = \sigma_{F_o}^{-2}$. At convergence, R was 0·139 and $wR = [\sum w(|F_o| - |F_c|)^2/\sum w|F_o|^2]^{1/2}$ was 0·055. For the subset of data with $I > 2{\cdot}3\sigma_I$, the values were 0·051 and 0·046. The error of fit was 1·24. $w\Delta^2$ was reasonably constant for ranges of F_o and $\sin\theta/\lambda$. A final difference map showed no unusual features. The refined value for the occupancy of Br at the 9 position was 0·613 (4). There was no evidence for split Br/C(methyl) positions or for disorder in the anthracene ring. Final atomic coordinates are shown in Table 1. Interatomic distances and angles are shown in Fig. 1.*

* Lists of structure factors and anisotropic thermal parameters have been deposited with the British Library Lending Division as Supplementary Publication No. SUP 36643 (9 pp.). Copies may be obtained through The Executive Secretary, International Union of Crystallography, 5 Abbey Square, Chester CH1 2HU, England.

Table 1. *Final fractional coordinates* ($\times 10^4$, *for* H $\times 10^3$) *and isotropic thermal parameters*

For non-hydrogen atoms $B_{eq} = \frac{8}{3}\pi^2 \sum_i \sum_j U_{ij} a_i^* a_j^* \mathbf{a}_i . \mathbf{a}_j$.

	x	y	z	B_{eq} or B (Å^2)
Br	−781 (1)	2149 (1)	2580 (3)	4·27
C(1)	−1329 (3)	3814 (4)	−764 (18)	3·91
C(2)	−1633 (4)	4502 (4)	−2248 (22)	4·91
C(3)	−1166 (4)	5162 (4)	−3312 (19)	4·85
C(4)	−405 (4)	5124 (3)	−2864 (20)	4·00
C(5)	1888 (3)	3605 (4)	1340 (19)	4·29
C(6)	2197 (4)	2934 (4)	2794 (22)	5·35
C(7)	1737 (4)	2268 (4)	3905 (20)	5·28
C(8)	961 (4)	2286 (4)	3357 (17)	4·40
C(9)	−180 (3)	3048 (3)	1279 (15)	3·17
C(10)	757 (3)	4371 (3)	−765 (14)	3·21
C(11)	−514 (3)	3743 (3)	−179 (14)	2·92
C(12)	−38 (3)	4424 (3)	−1300 (15)	3·07
C(13)	613 (3)	2990 (3)	1853 (14)	3·03
C(14)	1084 (3)	3674 (3)	769 (15)	3·14
C(15)	1373 (1)	5229 (1)	−1922 (5)	5·07
H(1)	−164 (3)	335 (3)	−8 (15)	3·67
H(2)	−221 (3)	460 (3)	−270 (19)	5·01
H(3)	−132 (3)	572 (4)	−431 (18)	5·35
H(4)	−12 (3)	553 (3)	−373 (18)	4·93
H(5)	217 (3)	399 (4)	40 (17)	4·67
H(6)	279 (4)	288 (3)	319 (18)	5·51
H(7)	196 (4)	182 (4)	489 (18)	5·46
H(8)	61 (3)	185 (3)	382 (16)	4·27

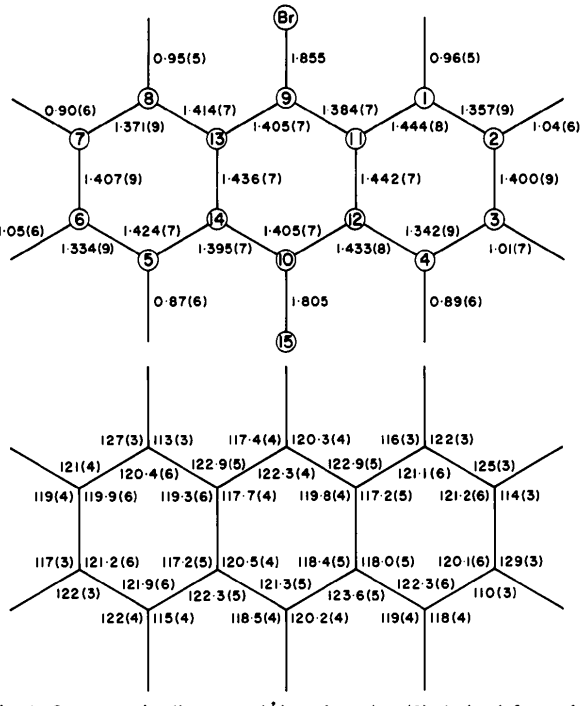

Fig. 1. Interatomic distances (Å) and angles (°) derived from the X-ray data. The e.s.d.'s are shown in parentheses.

Scattering factors were the analytical form tabulated in *International Tables for X-ray Crystallography* (1974). Anomalous-dispersion corrections for Br were taken from Cromer & Liberman (1970). Computer programs used were from the *ANUCRYS* structure determination package (P. O. Whimp, D. Taylor, G. M. McLaughlin and P. A. Kelly) and *SHELX* (Sheldrick, 1976).

Structure determination results and discussion

As expected the structure determination reveals that the molecule 9-bromo-10-methylanthracene is able to take up either of two orientations statistically throughout the crystal lattice. The determination further reveals that the two alternatives are not equally probable but that the site labelled Br in Table 1 is occupied on average by Br 61·3% and by methyl 38·7% while for the site labelled C(15) the percentages are reversed. Although we have not been able to confirm these figures with an independent measurement by neutron diffraction, our results for BMAR, for which both methods were employed, lead us to believe that such site occupancies are accurate to within 1%. On the basis of e.s.d.'s the occupancy factor for BMAN is marginally different from the value of 64·3% determined for BMAR (Jones & Welberry, 1980). It might be noted that we have also found similar site-occupancy values for the isomorphous chloro–methyl polymorphs CMAR (68·6%)

(Jones & Welberry, 1981) and CMAN (61·6%) but have no data at present on whether these values are dependent on the conditions of crystal growth. For a different compound (2,3-dichloro-6,7-dimethylanthracene) we have observed large differences in site-occupation factors for crystals grown from solution and by sublimation (Welberry, Jones & Epstein, 1982).

The structure determination does not reveal any unusual bond length or thermal parameters for the anthracene moiety, and the geometry parallels that found in pure anthracene (Mason, 1964; Lehmann & Pawley, 1972). Consequently we can conclude that to a very good approximation the disorder should be describable purely in terms of the 9,10 substituents. We chose to describe the 'average' electron density by allowing only one set of refineable positional parameters, for each substitution site, to avoid correlation problems. That the final refinement resulted in an acceptable R, no unusual parameter values, and a featureless difference map is considered reasonable justification for this model. The refined values for the Br—C(9) distance of 1·855 Å and for C(10)—C(15) of 1·805 Å lie between 1·897 Å for Br—C(aromatic) and 1·510 Å for C(methyl)—C(aromatic) [see Jones & Welberry (1980) for references]. It is interesting to note that using a weighted mean of these ideal bond lengths together with the observed site occupation yields values of 1·858 and 1·815 Å respectively. For calculation of intermolecular contact distances which we discuss in detail in a later section we therefore replaced the refined Br/Me with single Br or Me at the appropriate idealized distance from the anthracene moiety according to which of the alternative molecular orientations is assumed.

Diffuse scattering

In a previous paper (Welberry & Jones, 1980) we have reported a method of recording and interpreting diffuse-scattering data from molecular crystals. In this method long-exposure equi-inclination Weissenberg photographs are recorded and the resulting photographic image is processed by scanning and rewriting the data using an Optronics P1700 photomation system. By this means a background correction may be applied, the intensity enhanced to display the diffuse pattern more clearly, and the Weissenberg geometry removed. The final image corresponds to an undistorted view of a reciprocal-lattice section. This image is then compared with an optical diffraction pattern of a computer-generated model of the disordered structure, into which can be built statistical information of short-range ordering and thermal effects. While the model has its limitations, since an optical model can never perfectly represent atomic distributions, the method provides a rapid means of assessing at least semi-quantitatively the short-range-ordering effects in molecular crystals.

In the present case of BMAN it was evident from preliminary oscillation photographs that the diffuse scattering was largely concentrated in layers non-integral in l. Thus while information could be obtained from the optical-analogue method for $0kl$ and $h0l$ sections, the presence of these strong $hk\frac{1}{2}$ and $hk\frac{3}{2}$ layers was an incentive to develop a computer program to perform calculations of disorder diffuse scattering. Full details of these calculations will be reported elsewhere.

For both calculation and optical modelling we assumed initially that the disorder in BMAN involved molecules taking up one or other of two possible orientations at each molecular site. For simplicity we assumed that the anthracene moiety was unchanged on reversal and that the 9,10 substituents were placed at the refined positions irrespective of whether at the particular site the occupant was Br or Me. While the first assumption appeared to be justified by the crystal structure determination the second was justified by some preliminary tests which indicated that at the relatively low scattering angles we are dealing with, no consequences could be detected.

The two orientations of the molecule at the site x,y,z are assigned the labels (1) and (2). Operation of the space-group symmetry elements on these labels defines the labelling in the other molecular sites within the unit cell. Associated with each inter-site vector we define a correlation coefficient C_{ij}, where

$$C_{ij}=\frac{P(i=1,j=1)-P(i=1)^2}{P(i=1)\,P(i=2)}.$$

$P(i=1,j=1)$ is the joint probability that both sites i and j contain molecules in orientation (1) and $P(i=1)$ is the probability that site i contains a molecule in orientation (1). This latter is identified with the site occupancy discussed above. In our analysis of the diffuse X-ray pattern we attempt to assign values to the correlation coefficients associated with each intermolecular-site vector.

For BMAN we find that each molecule is in contact with 14 nearest neighbours but the vectors to these are not all unique. The environment of one molecule is shown in Fig. 2 and Table 2 and it will be seen that there are only seven independent nearest-neighbour vectors and all the others may be obtained by symmetry operations. Future reference to particular correlations will be in terms of the labelling A–G shown in Fig. 2.

While it might be expected that short-range ordering is practically entirely governed by nearest-neighbour interactions in molecular crystals because of the short range of the forces involved, that is not to say that higher-order (*i.e.* longer-range) correlations will not

Table 2. *The molecular environment*

For a central molecule at the x,y,z coordinates given in Table 1 the neighbouring molecules are specified as below.

Neighbour	At	Interaction label	Distance (Å) of molecular centres	Closest Br/Me (Å)
1	$x, y, 1+z$	*A*	3·96	3·96 (2×)
2	$x, y, -1+z$	*A*	3·96	3·96 (2×)
3	$-x, \frac{1}{2}+y, \frac{1}{2}-z$	*B*	8·28	3·68
4	$-x, -\frac{1}{2}+y, \frac{1}{2}-z$	*B*	8·28	3·68
5	$-x, \frac{1}{2}+y, -\frac{1}{2}-z$	*C*	8·37	3·95
6	$-x, -\frac{1}{2}+y, -\frac{1}{2}-z$	*C*	8·37	3·95
7	$\frac{1}{2}-x, 1-y, \frac{1}{2}+z$	*D*	8·98	4·46
8	$\frac{1}{2}-x, 1-y, -\frac{1}{2}+z$	*D*	8·98	4·46
9	$\frac{1}{2}+x, \frac{1}{2}-y, -z$	*E*	9·55	6·26
10	$-\frac{1}{2}+x, \frac{1}{2}-y, -z$	*E*	9·55	6·26
11	$\frac{1}{2}+x, \frac{1}{2}-y, 1-z$	*F*	10·26	7·27
12	$-\frac{1}{2}+x, \frac{1}{2}-y, 1-z$	*F*	10·26	7·27
13	$-\frac{1}{2}-x, 1-y, \frac{1}{2}+z$	*G*	10·75	>10
14	$-\frac{1}{2}-x, 1-y, -\frac{1}{2}+z$	*G*	10·75	>10

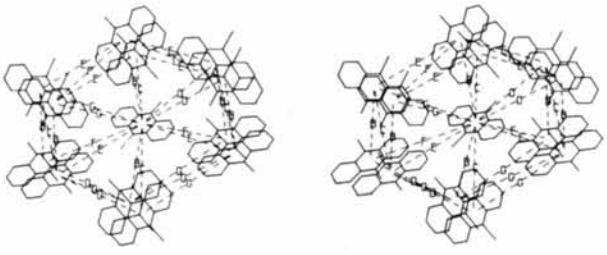

Fig. 2. Stereoscopic view of the molecular environment viewed approximately down **c**. In addition to the 12 molecular contacts shown the central molecule has '*A*'-type contacts with molecules translated by ±**c**. (See also Table 2.)

exist as an indirect consequence of two nearest-neighbour contacts with an intermediary, and some account must be taken of them. In the present work we suppose for calculation purposes that correlations to distant neighbours are given by the product of the primary correlations (A–G) along the most direct pathway to the molecule. Thus, for example, for the stack of molecules up the c axis whose primary correlation is A, second, third and fourth neighbours are assumed to be correlated by A^2, A^3, A^4. We shall refer to this in later sections as the 'product rule' for indirect correlations. This is equivalent to the adoption of the well known peak half-width determination of correlation coefficients given by Wilson (1962) and adopted, for example, by Flack (1970) and Glazer (1970). The optical-analogue models have this property in-built as a consequence of the way they are constructed (see Welberry, Miller & Pickard, 1979).

Determination of correlations

Although in general all correlations contribute to the diffuse scattering in an arbitrary reciprocal-lattice section the orientation of specific correlation vectors and the effects of symmetry mean that some sections are more favourable than others for the determination of particular correlations. For this reason an initial survey was carried out to discover which correlations contributed effectively to the four sections recorded. Despite the fact that intuitively the $hk\frac{1}{2}$ and $hk\frac{3}{2}$ sections promised to yield most information (since that was where most diffuse intensity lay), several of the correlations do not contribute to these sections. The vector A is normal to these planes and D and G do not contribute for the reason that contributions from

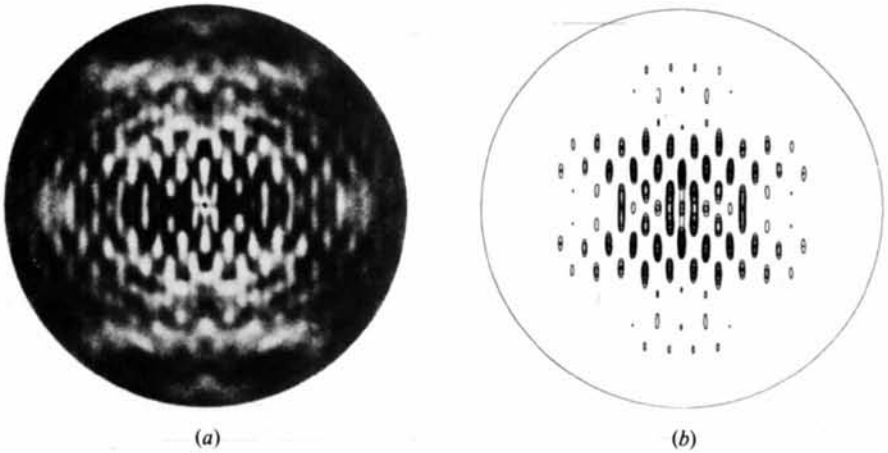

(*a*) (*b*)

Fig. 3. Diffuse scattering in the section $hk\frac{1}{2}$: (*a*) the X-ray data and (*b*) a computed intensity distribution in which correlations of $A = -0{\cdot}4$ and $C = +0{\cdot}4$ were used.

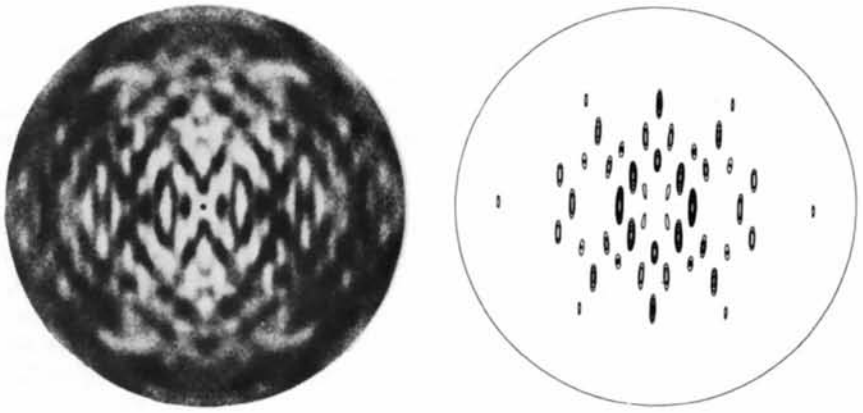

(*a*) (*b*)

Fig. 4. Diffuse scattering in the section $hk\frac{1}{2}$: (*a*) the X-ray data and (*b*) a computed intensity distribution in which correlations of $A = -0{\cdot}4$ and $C = +0{\cdot}4$ were used.

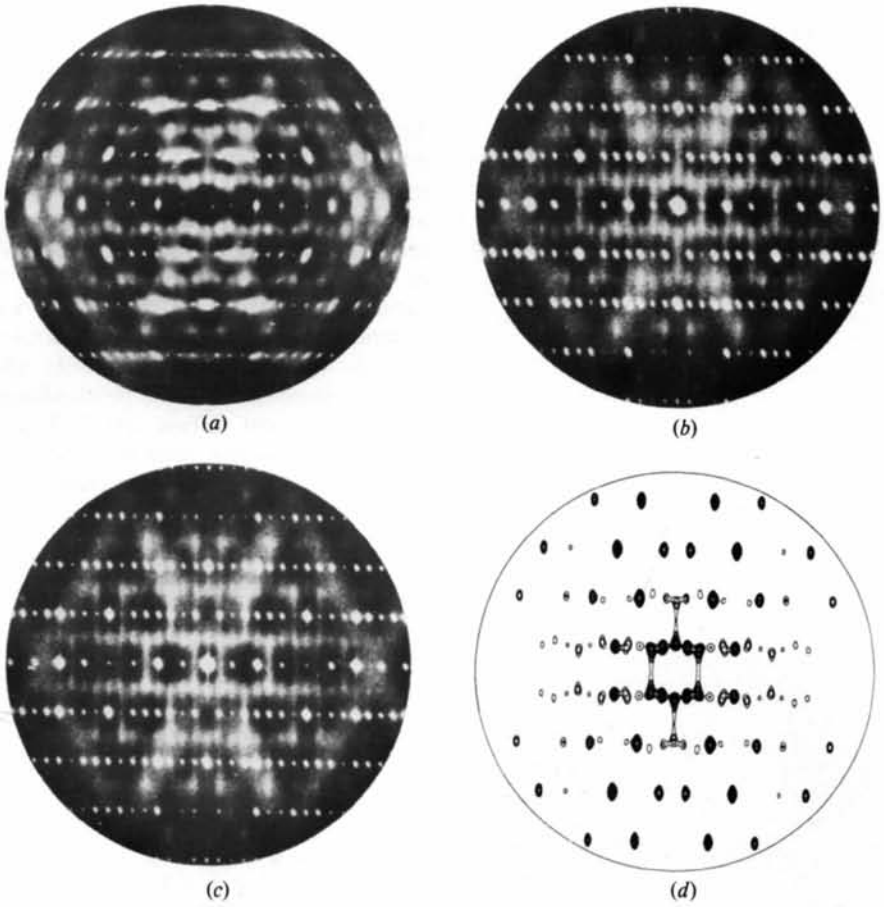

(*a*) (*b*) (*c*) (*d*)

Fig. 5. Diffuse scattering in the section $0kl$: (*a*) the X-ray data, (*b*) an optical simulation using the correlations $A = -0{\cdot}4$, $C = +0{\cdot}4$, (*c*) an optical simulation using $A = -0{\cdot}4$, $B = -0{\cdot}4$, and (*d*) a computed intensity distribution corresponding to (*b*).

symmetry-related vectors (see Fig. 2) cancel each other out. In addition correlations B and C cannot be distinguished since they give contributions which are identical although out of phase. That is to say if we observed a correlation in this section consistent with a given positive value of C it could equally well be produced by a negative value of B. In a similar way E and F cannot be distinguished. In principle the

problems can be resolved by consideration of the $0kl$ and $h0l$ sections since here all seven correlations can be distinguished.

Fig. 3 shows the X-ray pattern of the $hk\frac{1}{2}$ section together with the computed contour map which we considered was the best match. In this model we gave a value of 0·4 to C (or −0·4 to B) and 0·0 to E or F. In deciding the value of 0·4 we relied heavily on the inclusion of the higher-order terms C^2, C^3 *etc.* which critically alter the diffuse peak-profile width. Essentially the same correlation is present in Fig. 4 which is of the $hk\frac{1}{2}$ section. Here the computed pattern was made using the same value of 0·4 for C (or −0·4 for B) and no other correlation, and the agreement is equally satisfactory.

We next turn to the $0kl$ section to resolve the ambiguity between $-B$ and C. Fig. 5 shows optical simulations of this section produced with values of $C =$ 0·4 (Fig. 5*b*) and $B = -0{\cdot}4$ (Fig. 5*c*) together with a value of $A = -0{\cdot}4$ which we judged to be the best value for A based on its peak profile. Fig. 5(*d*) shows a computed contour map corresponding to the same correlation values as used in Fig. 5(*b*). No effect of thermal motion has been included in the computation, so the broad regions of thermal diffuse scatter observable in Fig. 5(*b*) and (*c*) are not present. Additionally, since no Debye–Waller factor has been applied to the scattering curves the disorder diffuse peaks at high angles are over-emphasized in this plot.

It is evident from this section that the simulation with $C = 0{\cdot}4$, $A = -0{\cdot}4$ shows good correspondence to the X-ray pattern (Fig. 5*a*) while that for $B = -0{\cdot}4$, $A = -0{\cdot}4$ does not. In this section also, we might expect to see contributions from D, E, F and G but we can find no evidence to suggest a significant contribution from any of them.

Turning finally to the $h0l$ section we show in Fig. 6 a comparison of the X-ray pattern with optical simulations using the same values of correlations used as those in Fig. 5. Here we see that both the $B = -0{\cdot}4$, $A = -0{\cdot}4$ case and the $C = 0{\cdot}4$, $A = -0{\cdot}4$ case show good correspondence to the X-ray pattern. However, the region marked by a 'Y' in the two simulations shows more intensity for the case of $C = 0{\cdot}4$, $A = -0{\cdot}4$

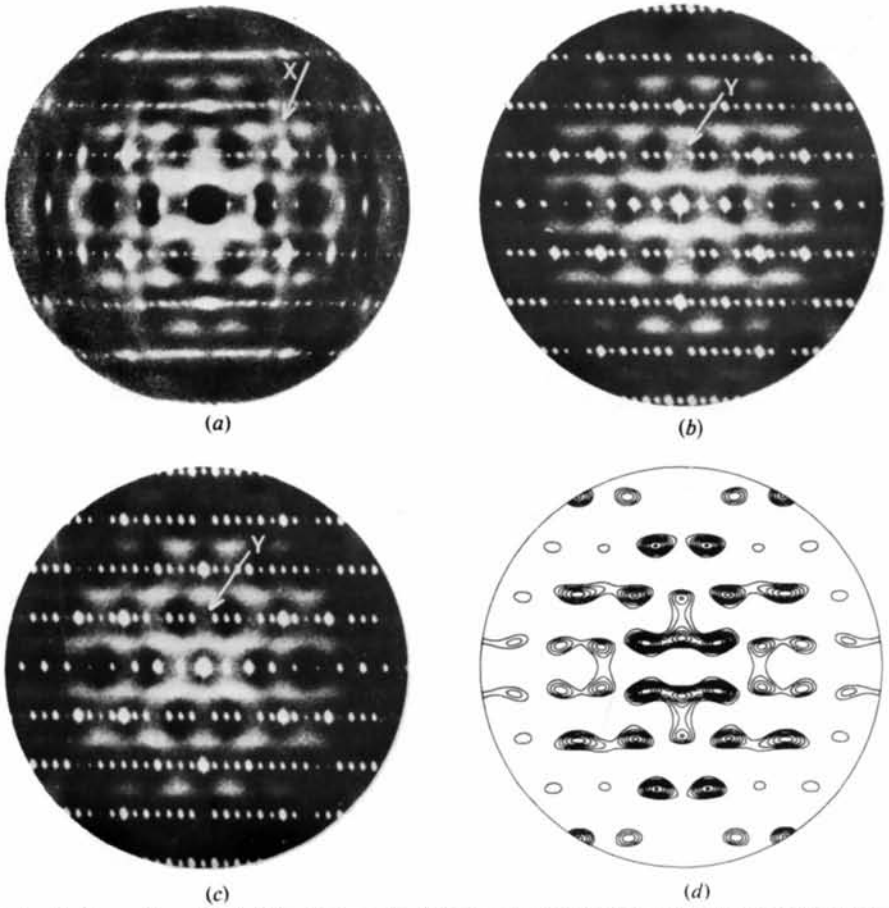

Fig. 6. Diffuse scattering in the section $h0l$: (*a*) the X-ray data, (*b*) an optical simulation using the correlations $A = -0{\cdot}4$, $C = +0{\cdot}4$, (*c*) an optical simulation using $A = -0{\cdot}4$, $B = -0{\cdot}4$, and (*d*) a computed intensity distribution corresponding to (*b*). For an explanation of the features marked 'X' and 'Y', see text.

to give better agreement. Fig. 6(*d*) shows a computed contour plot corresponding to the $C = 0{\cdot}4$, $A = -0{\cdot}4$ case.

One feature of the X-ray pattern of this section which is not reproduced in any of our models is a peak indicated by an 'X' in Fig. 6(*a*). We can find no short-range-order correlation which can account for this peak. There is some suggestion, since it appears between two strong thermal diffuse regions associated with Bragg peaks, that it may be of thermal or displacement-disorder origin. If this is the case then it represents a tendency towards cell-doubling and a possible phase transition. In this context it may be significant that on heating BMAN crystals appear to revert to BMAR crystals before decomposing.

It should be noted that since *A*, *B* and *C* form a triangle, application of the product rule for indirect correlations, mentioned previously, means that a value of $B = -0{\cdot}16$ is implicit when the prime correlation effects are $A = -0{\cdot}4$ and $C = +0{\cdot}4$. This value of *B* has been included in the optical simulations shown (of necessity) and in the calculations. Although in principle calculations may be made without this assumption, the assignment of independent values for indirect correlations would require a much more detailed and quantitative comparison of intensity distributions than our present methods can provide. Our present results seem to indicate that the product-rule assumption is not a bad one.

Discussion

Our results clearly indicate an ordering of the BMA molecules at two levels. Each individual molecular site has a greater chance of having in it the molecule in orientation (1), the occupation factor being about 61%. In addition there is short-range ordering such that molecules joined by either of the two vectors '*A*' and '*C*' have preferred mutual orientations. In Tables 3 and 4 we give details of these molecular contacts calculated using the idealized geometry discussed previously. Given in these tables are the distances for the four permutations of the orientations of the two molecules, and the relative frequency with which each occurs in the lattice. Also given for comparison are the frequencies for zero correlation; *i.e.* for a distribution having the same site occupancy but no short-range correlation. Note that the effect of the ordering is to reduce the number of Br–Br and C–C contacts and increase the number of Br–C contacts for both the '*A*' and '*C*' correlation.

Table 3. *Interactions for vector A* (*correlation* = −0·4)

Molecular orientations	Contact distance (Å)	Type of contact	Occurrence frequency	*cf.* frequency for zero correlation
1–1	3·96 3·96	Br–Br C–C	0·285	0·379
1–2	3·87 3·86	Br–C C–Br	0·331	0·237
2–1	4·09 4·08	Br–C C–Br	0·331	0·237
2–2	3·96 3·96	Br–Br C–C	0·053	0·147

Table 4. *Interactions of vector C* (*correlation* = +0·4)

Molecular orientations	Contact distance (Å)	Type of contact	Occurrence frequency	*cf.* zero correlation
1–1	4·07	C–Br	0·474	0·379
1–2	4·31	C–C	0·142	0·237
2–1	3·82	Br–Br	0·142	0·237
2–2	4·07	Br–C	0·242	0·147

Since this result is intuitively quite reasonable, in that we might expect the more electronegative Br atoms to prefer to be in contact with a methyl than another Br, it is somewhat surprising that the correlation '*B*' does not show the same marked trend. In Table 5 we show similar contact distances for the '*B*' correlation and frequencies based on the low negative correlation of −0·16. At present we cannot offer any simple explanation for this seeming anomaly, but can only conclude that since *A*, *B* and *C* form a triangle it is perhaps too simple-minded to consider each vector individually. For example it is evident that if '*B*' and '*C*' were both strong positive correlations then a strong negative correlation for *A* would be impossible.

Our aim in making measurements of short-range correlations in the type of molecular crystal described here is to extract information about the intermolecular forces involved in the formation of the crystal. While semi-empirical intermolecular-force calculations of the atom–atom 6 – exp type have proved very successful in predicting crystal structures and other properties of many compounds, particularly hydrocarbons (see *e.g.* Ramdas & Thomas, 1978), potentials for atoms as electronegative as Br have been less satisfactory. We have begun calculations using atom–atom potentials on disordered systems such as that described here and our initial results indicate that no tendency for short-range

Table 5. *Interactions for vector B* (*correlation* = −0·16)

Molecular orientations	Contact distance (Å)	Type of contact	Occurrence frequency	*cf.* zero correlation
1–1	3·79	C–Br	0·342	0·379
1–2	4·16	C–C	0·274	0·237
2–1	3·65	Br–Br	0·274	0·237
2–2	4·02	Br–C	0·110	0·147

ordering can be found using simple 6 – exp potentials such as those to be found for Br in Burgos & Bonadeo (1977) and C and H in Williams (1966). Our results indicate an approach in which additional electrostatic effects associated more locally with the Br and methyl groups would be more fruitful. One possibility is to include a dipole–dipole interaction as done, for example, by Reynolds (1975) for the carbonyl dipole in anthrone, and we are proceeding along these lines. Work is in progress on a number of similar compounds involving disorder between Br and methyl substituents.

We are grateful to M. Puza for the preparation of the material used in this work.

References

BURGOS, E. & BONADEO, H. (1977). *Chem. Phys. Lett.* **49**, 475–478.

CROMER, D. T. & LIBERMAN, D. (1970). *J. Chem. Phys.* **53**, 1891–1898.

ELCOMBE, M. M., COX, G. W., PRYOR, A. W. & MOORE, F. H. (1971). *Programs for the Management and Processing of Neutron Diffraction Data.* Report AAEC/TM578. Australian Atomic Energy Commission.

FLACK, H. D. (1970). *Philos. Trans. R. Soc. London Ser. A*, **266**, 559–591.

GLAZER, A. M. (1970). *Philos. Trans. R. Soc. London Ser. A*, **266**, 593–639.

HELLER, E. & SCHMIDT, G. M. J. (1971). *Isr. J. Chem.* **9**, 449–462.

International Tables for X-ray Crystallography (1974). Vol. IV. Birmingham: Kynoch Press.

JONES, R. D. G. & WELBERRY, T. R. (1980). *Acta Cryst.* B**36**, 852–857.

JONES, R. D. G. & WELBERRY, T. R. (1981). *Acta Cryst.* B**37**, 1125–1126.

LEHMANN, M. S. & PAWLEY, G. S. (1972). *Acta Chem. Scand.* **26**, 1996–2004.

MASON, R. (1964). *Acta Cryst.* **17**, 547–555.

MOORE, F. H. (1972). *Acta Cryst.* A**28**, S256.

PRAT, M. T. (1961). *Acta Cryst.* **14**, 110–112.

RAMDAS, S. & THOMAS, J. M. (1978). *Chem. Phys. Solids Surfaces*, **7**, 31–58.

REYNOLDS, P. A. (1975). *Acta Cryst.* A**31**, 80–83.

SHELDRICK, G. M. (1976) *SHELX.* A program for crystal structure determination. Univ. of Cambridge, England.

WELBERRY, T. R. & JONES, R. D. G. (1980). *J. Appl. Cryst.* **13**, 244–251.

WELBERRY, T. R., JONES, R. D. G. & EPSTEIN, J. (1982). To be published.

WELBERRY, T. R., MILLER, G. H. & PICKARD, D. K. (1979). *Proc. R. Soc. London Ser. A*, **367**, 175–192.

WILLIAMS, D. E. (1966). *J. Chem. Phys.* **45**, 3770–3778.

WILSON, A. J. C. (1962). *X-ray Optics.* London: Methuen.

Acta Cryst. (1982). B**38**, 1525–1529

2-[3-(*o*-Nitrophenylthio)-1-indenylidene]-1,3-dithiolane, 2-[3-(*o*-Nitrophenylthio)-1-indenylidene]-1,3-dithiole and 2-{3-[1-(1,3-Dithiolan-2-ylidene)-2,3-dihydro-2-indenyl]-1-indenylidene}-1,3-dithiolane

BY JOHN C. BARNES AND JOHN D. PATON

Chemistry Department, The University, Dundee DD1 4HN, Scotland

AND BRIAN H. NICHOLLS

The Wakeman School, Shrewsbury, Shropshire, England

(*Received* 5 *August* 1981; *accepted* 3 *December* 1981)

Abstract

The crystal and molecular structures of the title compounds have been determined. (I) $C_{18}H_{13}NO_2S_3$ is monoclinic, space group $P2_1/c$ with $a = 11{\cdot}584$ (6), $b = 10{\cdot}935$ (7), $c = 16{\cdot}173$ (8) Å, $\beta = 121{\cdot}5$ (3)°, $U = 1746$ Å^3, $Z = 4$, $D_c = 1{\cdot}36$ g cm^{-3}, $F(000) = 768$, μ(Cu $K\alpha$) = 38 cm^{-1}. (II) $C_{18}H_{11}NO_2S_3$ is triclinic, space group $P\bar{1}$, with $a = 10{\cdot}782$ (5), $b = 8{\cdot}40$ (1), $c = 10{\cdot}501$ (6) Å, $\alpha = 107{\cdot}95$ (5), $\beta = 69{\cdot}23$ (1), $\gamma = 109{\cdot}0$ (1)°, $U = 820{\cdot}6$ Å^3, $Z = 2$, $D_c = 1{\cdot}40$ g cm^{-3}, $F(000) = 380$, μ(Cu $K\alpha$) = 41 cm^{-1}. (III) $C_{24}H_{20}S_4$ is monoclinic, space group $P2_1/n$, with $a = 12{\cdot}23$ (1), $b = 7{\cdot}58$ (1), $c = 23{\cdot}43$ (2) Å, $\beta = 105{\cdot}96$°, $U = 2088{\cdot}6$ Å^3, $Z = 4$, $D_c = 1{\cdot}39$ g cm^{-3}, $F(000) = 912$, μ(Cu $K\alpha$) = 40 cm^{-1}. Refinement for (I), (II) and (III) converged at $R = 0{\cdot}047$, 0·069 and 0·057 for, respectively, 1852, 1486 and 1600 unique reflexions above background.

0567-7408/82/051525-05$01.00